/N-34-CR
116631
P.38

Center for Stirling Technology Research
Ohio University, Athens, OH

Oscillating-Flow Regenerator Test Rig: Woven Screen and Metal Felt Results

D. Gedeon

Gedeon Associates
Athens, OH

J.G. Wood

Center for Stirling Technology Research
Ohio University
Athens, OH

July 29, 1992

Center for Stirling Technology Research
Ohio University, Athens, OH

Oscillating-Flow Regenerator Test Rig: Woven Screen and Metal Felt Results

D. Gedeon

Gedeon Associates
Athens, OH

J.G. Wood

Center for Stirling Technology Research
Ohio University
Athens, OH

July 29, 1992

Contents

Abstract

In which we present correlating expressions, in terms of Reynolds or Peclet numbers, for friction factors, Nusselt numbers, enhanced axial conduction ratios and overall heat flux ratios in four porous regenerator samples representative of stirling-cycle regenerators: two woven screen samples and two random wire samples. Error estimates and comparison with data of others suggest our correlations are reliable, but we need to test more samples over a range of porosities before our results will become generally useful.

1 The Continuing Saga

This report brings together into one document combined pressure-drop and heat-transfer results for the first set of four samples exhaustively tested on the OU/CSTR (Ohio University Center for Stirling Technology Research) Oscillating-flow regenerator test rig. Pressure-drop results were previously reported in an internal memo *Regenerator Test Rig: More Results — Part 1*, dated March 31, 1992. Heat-transfer results were outlined in a handout *CSTR/OU Regenerator Oscillating-Flow Test Rig Results*, presented at the NASA-Lewis Stirling Loss Understanding Workshop June 3, 1992. Said outline has been somewhat corrected and considerably amplified in this report.

The last generally available report pertaining to this test rig was the Sunpower SBIR phase I final report [4]. Although that report remains valid so far as experimental goals and data reduction methodology, both hardware and software have evolved significantly since it was written. A running series of internal memos have documenting many of these changes, but the memos have not always been widely disseminated, nor do they offer the most concise possible statement of the current state of affairs. As we now seem to be fairly well along on the evolutionary path, it is probably safe to attempt a brief summary at this time of the highlights of test rig development.

In this spirit, we offer the following chronology of key events in our test rig's history since the time of final report [4]. The dates given correspond to dates on various internal memos, reports and log-book entries. Eventually, when all experimental work is complete, we hope to supersede the present report with the mother of all final reports (or book?) tying everything together in great detail — theory, hardware and test results.

July 27, 1990 We decide to use GLIMPS simulation of each experimental data point to determine the non-measured experimental variable g (sample mass flux rate) as a Fourier time-series. Thus, GLIMPS simulation, automatically adjusted under the GLOP umbrella to match key experimental measurements, becomes an integral part of our data reduction process. GLIMPS is a commercial software package for stirling machine simulation and GLOP is its optimization driver.

July 30, 1990 In innocence we suggest it would be a good idea to do pressure-drop testing on our samples at the same time as heat-transfer testing. Accordingly, we develop a procedure for reducing friction factors from pumping dissipation measurements. Pressure-drop testing soon becomes the law of the land.

July 31, 1990 Because of plumbing nightmares and safety concerns, we abandon the oil-heated shell-and-tube heater and replace it with a much simpler electrically heated copper block having drilled-hole gas passages.

August 6, 1990 We notice it is a simple matter to reduce an overall-heat-flux dimensionless group N_q from our heat-transfer testing. Why not? N_q modeling also becomes standard.

April 11, 1991 We decide to change coolant temperature transducers from thermocouples to thermistors to improve ΔT measurement accuracy.

July 24, 1991 We size a capillary line for test-section pressure-equalization during charging and discharging — big enough for reasonable charge time but small enough not to affect experimental measurements.

August 29, 1991 We trace bad thermocouple readings to a manufacturing flaw in the instrumentation submultiplexer board. A resistor substitution fixes the problem.

December 13, 1991 We complete our first shake-down pressure-drop and heat-transfer tests. Correlations are promising but error bands are large due to limited Reynolds number range, small number of data points logged and other hardware and software troubles. It becomes apparent that we should do pressure-drop testing separately, with the sample only attached to the piston cylinder (no cooler, heater, diffuser disks). And we uncover a number of bugs in our data acquisition and reduction techniques.

March 31, 1992 We scrap the labor intensive and non-repeatable molded rubber sample holder in favor of a more modular equivalent with test sample shrink-fitted into a Torlon cylinder, then o-ring sealed to separate and permanent diffuser disk / thermocouple assemblies. Improved graphical and tabular outputs find their way into the data reduction software, which becomes more friendly to humans and easier to maintain.

March 31, 1992 We complete exhaustive pressure-drop testing on our first four samples. Results look very good. We also hurry through preliminary heat-transfer tests, which seem to suffer from large and erratic static conduction values. We postpone further testing while investigating the problem. Eventually, we improve heater insulation and decide to run the rig upside down (heater on top) to minimize convective heat transfer between heater and cooler.

2

May 27, 1992 Erratic static conduction, though smaller now, remains our chief bug-a-boo. Rather than measuring static conduction just once up-front, we decide to measure it several times within each data set by simply logging zero-piston-amplitude points and letting the data reduction software deal with it. Thus we recognize a formal data screening step in the data reduction process in which .RAW files become .SCN files before further processing.

May 30, 1992 We complete exhaustive heat-transfer testing for our four samples in time to present results at the NASA Loss Workshop. Things look pretty good at this time but yet-to-be-discovered problems with error estimation screw up simultaneous reduction of Nusselt number and enhanced axial-conductivity ratio.

June 17, 1992 Feedback from the NASA loss workshop leads us to revise our error estimates for sample temperature gradient.

Since the last entry, we have gone over our heat-transfer test data more carefully, removing questionable data points and adding some that were previously omitted for reasons too complicated to dwell on. We have also corrected a software error that persistently overestimated coolant thermistor error in the high R_e range, thereby weighting our parameter estimates toward the low R_e range. Thus the heat-transfer results in this report look much better than previously reported.

2   Samples Tested

We have tested four samples under this effort, chosen as representatives of typical regenerator matrices used in modern stirling machines:

stacked screens 200 mesh (per inch) stainless steel woven wire screens packed individually into sample holder, wire diameter 53.3 microns (0.0021 in), porosity 0.6328, sample thickness 11.1 mm

sintered screens nominally the same screens but this time sintered, porosity 0.6232, sample thickness 10.1 mm

Brunswick 1 Brunswick stainless steel sintered metal felt, round wire 25.4 micron (0.001 in) diameter, porosity 0.8233, sample thickness 12.9 mm

Brunswick 2 Brunswick stainless steel sintered metal felt, round wire 12.7 micron (0.0005 in) diameter, porosity 0.8405, sample thickness 14.9 mm

3 Nomenclature

The following symbols are those appropriate for a computational model of porous regenerator flow where the computational grid is large compared to the matrix pore size. Accordingly, thermodynamic variables like T, u, etc., are understood in a local-average sense — spatially averaged over a large enough volume to remove eddy fluctuations, yet still small compared to the overall problem dimensions. This viewpoint is consistent with the measurement resolution in the test rig itself.

c_p gas specific heat at constant pressure

d_h hydraulic diameter: $d_h = 4/s$

g mass flow rate per unit void area: ρu

g_m peak value of g

h heat transfer coefficient between gas and solid matrix

h_e effective heat transfer coefficient that includes the effects of k_a when used in an oscillating-flow regenerator model

k molecular gas conductivity

k_a apparent agitated-flow gas axial conductivity (based on mean void flow area)

L test-sample length

P pressure

q_h part of q_t attributed to enthalpy transport (finite h)

q_k part of q_t attributed to apparent axial conduction

q_t time-average total energy flux (per unit void area) down the regenerator

q_t^* q_t, less static conduction

s matrix surface area per unit void volume

t time

T gas temperature (local void average)

T_s solid matrix temperature (local solid average)

u gas velocity (local void average)

x axial coordinate

μ molecular gas viscosity (local void average)

ρ gas density (local void average)

ω angular frequency (rad/s)

Dimensionless Groupings

f Darcy friction factor: $d_h \frac{\partial P}{\partial x}/(\rho \frac{u|u|}{2})$

N_k axial conductivity enhancement ratio: $\frac{k_a}{k}$

N_{k0} value of N_k at static flow conditions

N_u Nusselt number: $\frac{h d_h}{k}$

N_{ue} effective Nusselt number: $\frac{h_e d_h}{k}$

N_q overall heat flux ratio: $q_i^*/(k\frac{\partial T}{\partial x})$

P_e Peclet number: $R_e P_r$

P_{em} peak Peclet number: $R_{em} P_r$

P_r Prandtl number: $\frac{\mu c_x}{k}$

R_e Reynolds number: $\frac{g d_h}{\mu}$

R_{em} peak Reynolds number: $\frac{g_m d_h}{\mu}$

V_a Valensi number: $\frac{\rho \omega d_h}{4\mu}$

δ/L tidal amplitude ratio: $g_m/(\rho \omega L) = (d_h/(4L)) R_{em}/V_a$

Subscripts

0   static-flow value

m peak value (amplitude of first harmonic)

Operators

{ }   time average over one cycle: $\{f\} = \frac{\omega}{2\pi} \int_0^{2\pi/\omega} f dt$

4   Summary of Final Correlations

We begin with a collection of correlating expressions for our four test samples which will enable stirling-cycle modelers to calculate regenerator pressure-drop and thermal-loss (heat-transfer) characteristics from mean flow variables. Readers new to the distinctions between N_u, N_k and N_{ue} in stirling modeling will want to study section 5 of this report.

4.1   Friction Factors

We modeled Darcy friction factors in the form

$$f = a_1/R_e + a_2 \tag{1}$$

where a_1 and a_2 appear in the following table for the various materials tested. The plus-and-minus tolerances reflect the 90% confidence intervals calculated by the parameter estimating software.
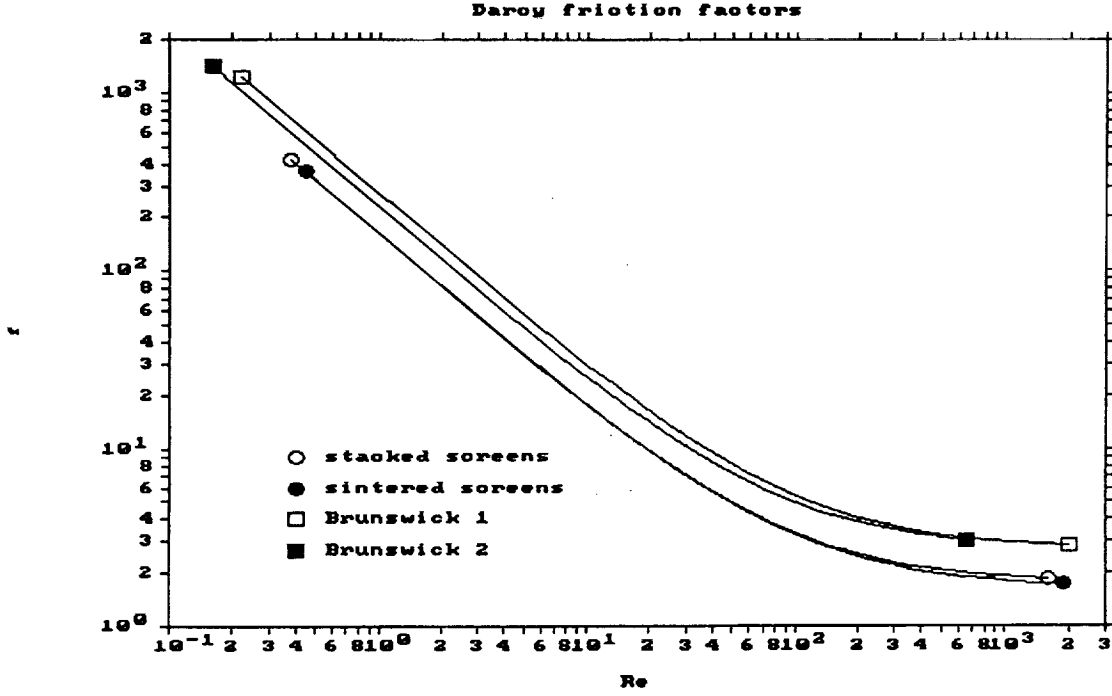
5

Figure 1: Oscillating-flow friction factors for the four test samples

	stacked screens	sintered screens	Brunswick 1	Brunswick 2
a_1	159 ± 6	162 ± 6	271 ± 8	226 ± 4
a_2	1.74 ± 0.008	1.64 ± 0.016	2.71 ± 0.015	2.69 ± 0.039
R_{em} range	$0.38 - 1600$	$0.45 - 1900$	$0.22 - 2050$	$0.16 - 665$
V_a range	$0.0058 - 3.7$	$0.0044 - 3.3$	$0.0050 - 5.6$	$0.0016 - 1.4$
δ/L range	$0.10 - 2.0$	$0.20 - 2.3$	$0.091 - 1.4$	$0.077 - 1.2$

The above correlations are plotted in figure 1.

The chosen equation form is based on the well-known Ergun equation popular in the engineering literature [10]. Roughly, the Ergun equation implies creeping-viscous-dominated Darcy flow for low R_e, where a_1/R_e dominates, smoothly transitioning to turbulent-like flow at high R_e, where a_2 dominates. The asymptotic approach to $f = a_2$ is roughly consistent with cylinder drag coefficients, as tabulated on p. 214 of Holman [6], at least up until a sharp drop-off at $R_e \approx 10^5$ where stirling regenerators are unlikely to operate.

6

4.2 Overall Heat Flux Ratios

So far as we know, the notion of overall heat flux ratio is new. The idea is that we can correlate the overall thermal loss down a stirling-cycle regenerator by a simple expression in terms of the peak Peclet number. We modeled overall heat flux ratio (measured net heat flux above static conduction / molecular gas conduction down equivalent void area) in the form

$$N_q = a_1 P_{em}^{a_2}$$

Note that Peclet number is the *peak* not instantaneous value. Parameters a_1, a_2 and their 90% confidence intervals appear in the following table:

	stacked screens	sintered screens	Brunswick 1	Brunswick 2
a_1	0.34 ± 0.03	0.40 ± 0.02	0.29 ± 0.02	0.42 ± 0.05
a_2	1.35 ± 0.01	1.32 ± 0.01	1.31 ± 0.01	1.23 ± 0.02
R_{em} range	$1.23 - 1010$	$4.75 - 1100$	$1.61 - 996$	$2.58 - 468$
V_a range	$0.0088 - 1.7$	$0.0059 - 1.7$	$0.015 - 2.5$	$0.013 - 0.93$
δ/L range	$0.22 - 2.5$	$0.32 - 3.0$	$0.21 - 1.8$	$0.15 - 1.6$

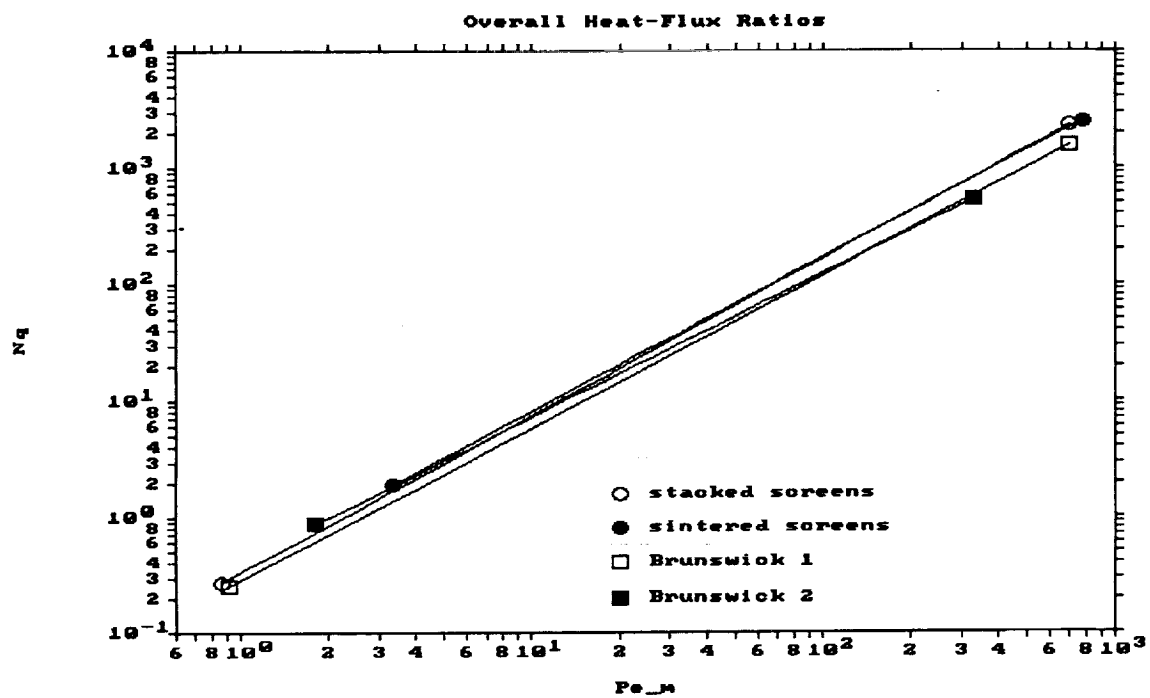The above correlations are plotted in figure 2.

Figure 2: Overall heat flux ratios for the four test samples

8

4.3 N_u and N_k Simultaneously

Nusselt numbers and enhanced conductivity ratios as presented here should be used together in an oscillating-flow regenerator model that simultaneously includes the effects of both film heat transfer and enhanced axial conduction. Since they are based on best estimates of the true regenerator physics, they may also be used with caution by porous flow modelers in other fields. The presumed correlating expressions are

$$N_u = a_1 P_e^{a_2} \tag{2}$$

$$N_k - N_{k0} = a_3 P_e^{a_2} \tag{3}$$

where parameters a_1 through a_3 and their 90% confidence intervals appear in the following table:

	stacked screens	sintered screens	Brunswick 1	Brunswick 2
a_1	0.62 ± 0.10	0.57 ± 0.09	0.64 ± 0.11	0.50 ± 0.25
a_2	0.60 ± 0.03	0.62 ± 0.03	0.65 ± 0.03	0.71 ± 0.08
a_3	1.24 ± 0.51	1.70 ± 0.69	0.56 ± 0.42	0.60 ± 0.87
R_{em} range	$1.23 - 1010$	$4.75 - 1100$	$1.61 - 996$	$2.58 - 468$
V_a range	$0.0088 - 1.7$	$0.0059 - 1.7$	$0.015 - 2.5$	$0.013 - 0.93$
δ/L range	$0.22 - 2.5$	$0.32 - 3.0$	$0.21 - 1.8$	$0.15 - 1.6$

The above correlations are plotted in figure 3.

Enhanced Axial Conductivity Ratios
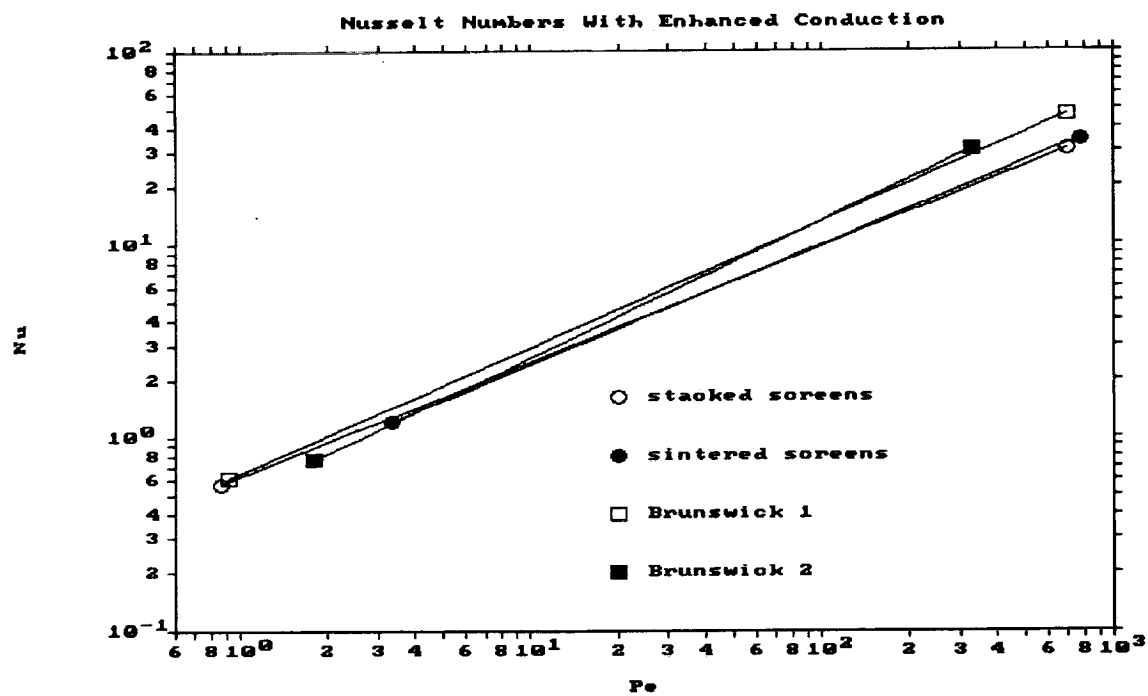
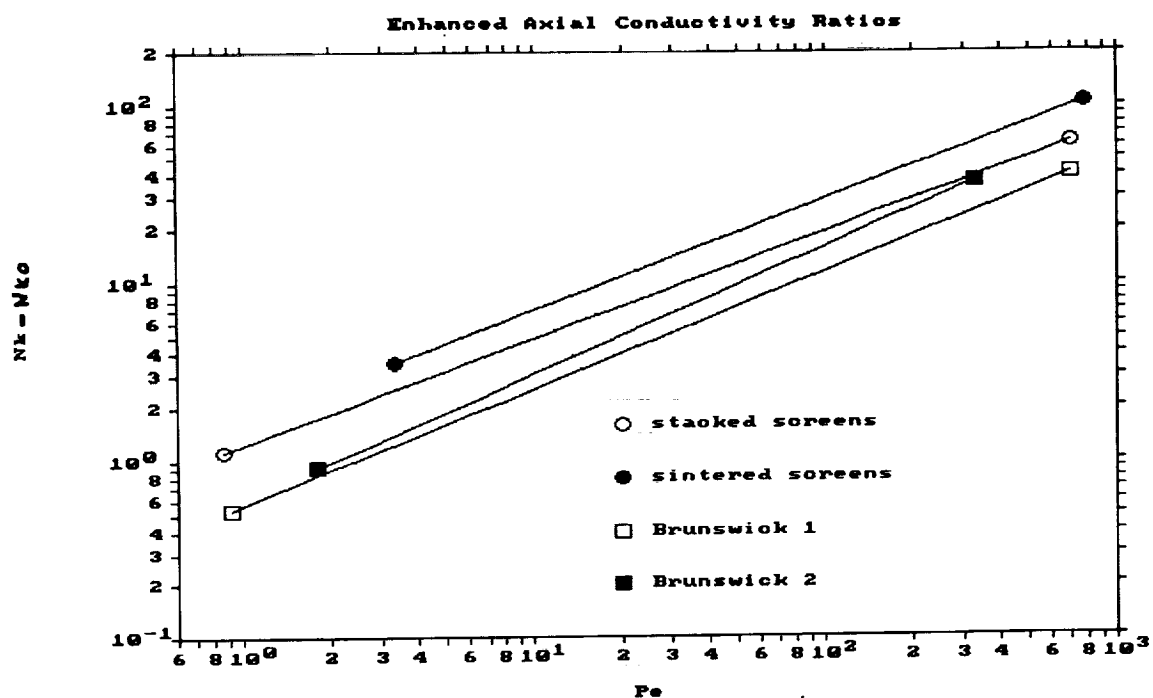**Nusselt Numbers With Enhanced Conduction**

Figure 3: Simultaneously modeled Nusselt numbers and enhanced axial conductivity ratios for the four test samples

10

4.4 N_{ue} assuming $N_k = N_{k0}$

Effective Nusselt number N_{ue} captures the total oscillating-flow regenerator heat flux q_t^* in enthalpy transport alone. We intended it for use primarily by stirling modelers who prefer to neglect enhanced axial conduction. In other applications it will tend to under-predict actual film heat transfer for a given temperature difference — especially at Peclet numbers below about 10. The presumed correlating expressions are

$$N_{ue} = a_1 P_e^{a_2} \tag{4}$$
$$N_k - N_{k0} = 0 \tag{5}$$

where parameters a_1 and a_2 and their 90% confidence intervals appear in the following table:

	stacked screens	sintered screens	Brunswick 1	Brunswick 2
a_1	0.43 ± 0.04	0.37 ± 0.02	0.51 ± 0.03	0.35 ± 0.04
a_2	0.65 ± 0.01	0.68 ± 0.01	0.69 ± 0.01	0.77 ± 0.02
R_{em} range	$1.23 - 1010$	$4.75 - 1100$	$1.61 - 996$	$2.58 - 468$
V_a range	$0.0088 - 1.7$	$0.0059 - 1.7$	$0.015 - 2.5$	$0.013 - 0.93$
δ/L range	$0.22 - 2.5$	$0.32 - 3.0$	$0.21 - 1.8$	$0.15 - 1.6$

The narrower confidence bands this time reflect the comparative ease of modeling two rather than three parameters, not any intrinsic superiority of the world view neglecting enhanced axial conduction. In fact, the previous three-parameter modeling for simultaneous N_u and N_k gave a slightly but significantly better fit to the data, as measured by the minimum chi-squared value of the residuals. The above correlation is plotted in figure 4.
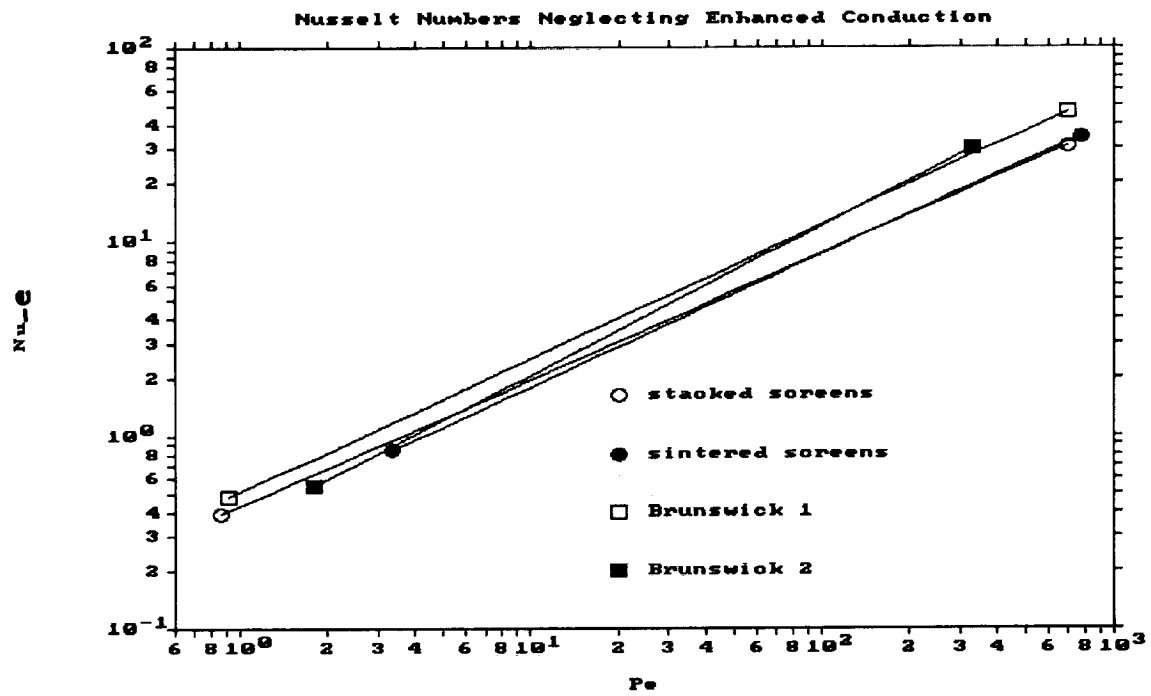
Figure 4: Effective Nusselt numbers neglecting enhanced axial conduction, for the four test samples

12

5   Enthalpy Transport vs Enhanced Axial Conduction

We and others have identified two distinct processes of thermal energy transport important in porous regenerators: enhanced gas axial conduction (compared to molecular conduction) and enhanced film heat transfer between the gas and the solid matrix (compared to laminar-flow film heat transfer). Both processes contribute to net thermal energy transport down the regenerator — axial thermal diffusion directly and film heat transfer via net enthalpy transport. The same microscopic fluctuations of the porous-flow velocity and temperature fields drive both processes (similar to the way turbulent velocity fluctuations drive the analogous processes in duct flows). So both processes are equally real.

We must emphasize this last point because many stirling engineers remain reluctant to accept the notion of enhanced thermal diffusion in porous flows. This is somewhat perplexing in light of their acceptance of enhanced conduction in turbulent flows. And it is even more perplexing in light of the large number of papers on the topic in the chemical engineering field (see [3], for example), and more recently the paper co-authored by mechanical engineer Ping Cheng [2], who bore witness on the matter at the 1992 NASA Stirling Loss Workshop.

At any rate, we herein recognize the existence of both enhanced thermal diffusion and film heat transfer. The problem is, our test rig is unable to distinguish the two in absolute terms. This is because our primary measurable is net regenerator heat flux, into which both processes are thoroughly mixed.

However, it turns out that we can distinguish between the two fundamental processes given some advance assumptions about the functional form of their correlating expressions. Let me explain. We correlate enhanced axial conduction in terms of dimensionless group N_k which theoretical arguments suggest is some function of Peclet number. N_k may also be a function of other dimensionless groupings, but it will turn out that these may be neglected in the range of our tests. Likewise, we correlate film heat transfer in terms of Nusselt number N_u, also a function of Peclet number only. If this is all we knew, our test rig would be powerless to resolve either one. However, we are led by tradition to presume the validity of power-law correlations (the kind that plot as straight lines on log-log plots), at least a over a limited range of Peclet numbers. Furthermore, we can argue that since the underlying enhancement mechanism is the same for both N_k and N_u, the correlating exponents for both must be the same (or nearly the same) [5]. Thus we wind up with three parameters, $a_1 - a_3$, to be determined in the correlating expressions (2) and (3). The previous error-estimate tables show us that presuming these functional forms is sufficient for us to simultaneously determine both N_u and N_k from our data — to within a reasonable degree of confidence.

On the other hand, out of deference to stirling tradition, we can choose to ignore enhanced axial conduction completely and still reduce an effective Nusselt

number from our data. The N_{u_e} so obtained is different from the previous one, but equally valid for stirling research purposes so long as we apply it consistently in any computational model. In this method we estimate just a_1 and a_2 in the expressions (4) and (5). In terms of this N_{u_e} we will get the correct thermal energy transport down our regenerator, but solely in terms of net enthalpy transport, without any enhanced thermal diffusion.

Of course the distinction between N_u and N_{u_e} may be more critical in other fields of science or engineering. For example, if we really did need to know the film heat transfer between the porous solid and the gas (a reactor cooling problem?) then our second N_{u_e} form of Nusselt number will certainly give the wrong answer. Our first form could also give the wrong answer if our presumed functional forms are incorrect, but it does seem more likely to be correct. Thus we caution against 100% confidence in applying our results to non-stirling fields, but if pressed, would recommend the form where both N_u and N_k are considered simultaneously.

Careful readers will have noted that the confidence bands for parameter a_3 in the above tables (the coefficient for N_k) were rather large. We can get an idea why this is so and a feel for its significance by looking into the individual contributions of N_u and N_k to the total thermal energy flux down the regenerator. This was all worked out in the SBIR phase I report [4]. N_u contributes by way of net enthalpy transport per unit void area

$$q_h = \{c_p g T\} \tag{6}$$

where the $\{\}$ operator denotes time average. N_k contributes by way of enhanced axial conduction per unit void area

$$q_k = -\frac{\partial T}{\partial x}\{k_a\} \tag{7}$$

Section 4.2.4 of the SBIR phase I report derives the following expression for q_h and q_k in terms of the previous functional forms (2) and (3) for N_u and N_k, also presuming sinusoidal oscillating mass flux g:

$$q_h = -k\frac{\partial T}{\partial x}\frac{1}{4a_1}P_{em}^{2-a_2}\left\{|\sin|^{2-a_2}\right\} \tag{8}$$

$$q_k - q_{k0} = -k\frac{\partial T}{\partial x}a_3 P_{em}^{a_2}\left\{|\sin|^{a_2}\right\} \tag{9}$$

figure 5 plots both q_h and $q_k - q_{k0}$ as functions of peak Peclet number for our four samples. We see that enthalpy transport q_h dominates over most of the Peclet number range, with increasing dominance as Peclet number increases. This would account for the relatively large error band for parameter a_3 in the N_k correlation. There is a cross-over point, somewhere in the range $P_{em} \approx 3\text{-}6$, where enthalpy transport is about equal to enhanced axial conduction. Below this cross-over point, enhanced axial conduction dominates, but the magnitude of the enhancement is small, only a slight increase over molecular conduction.
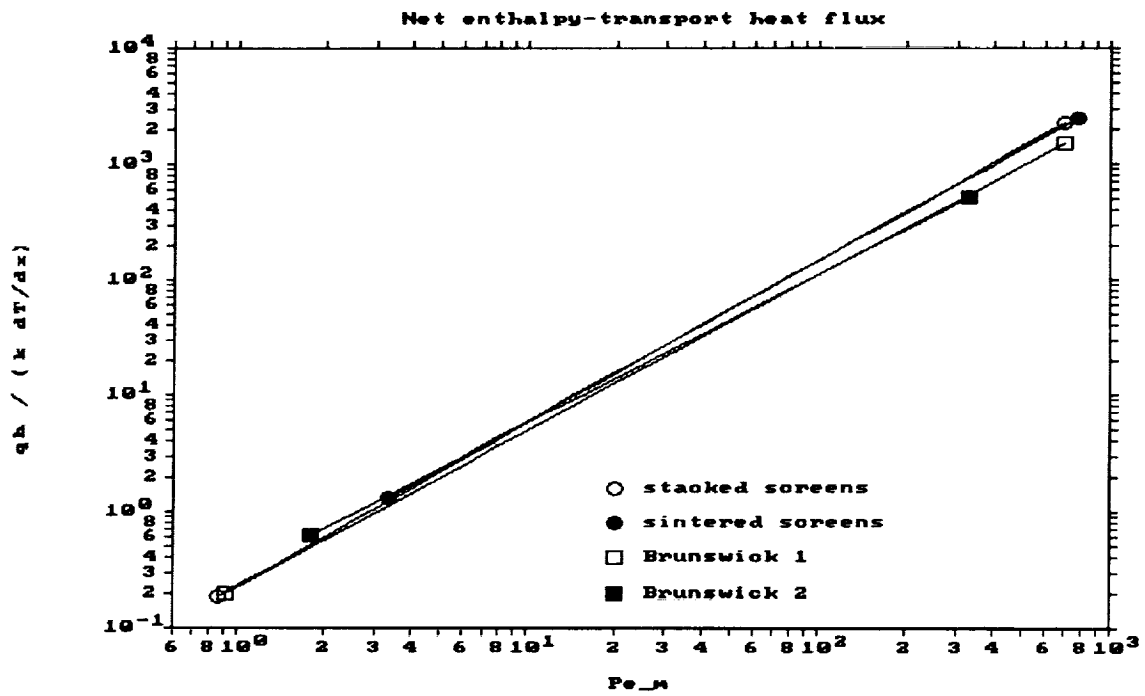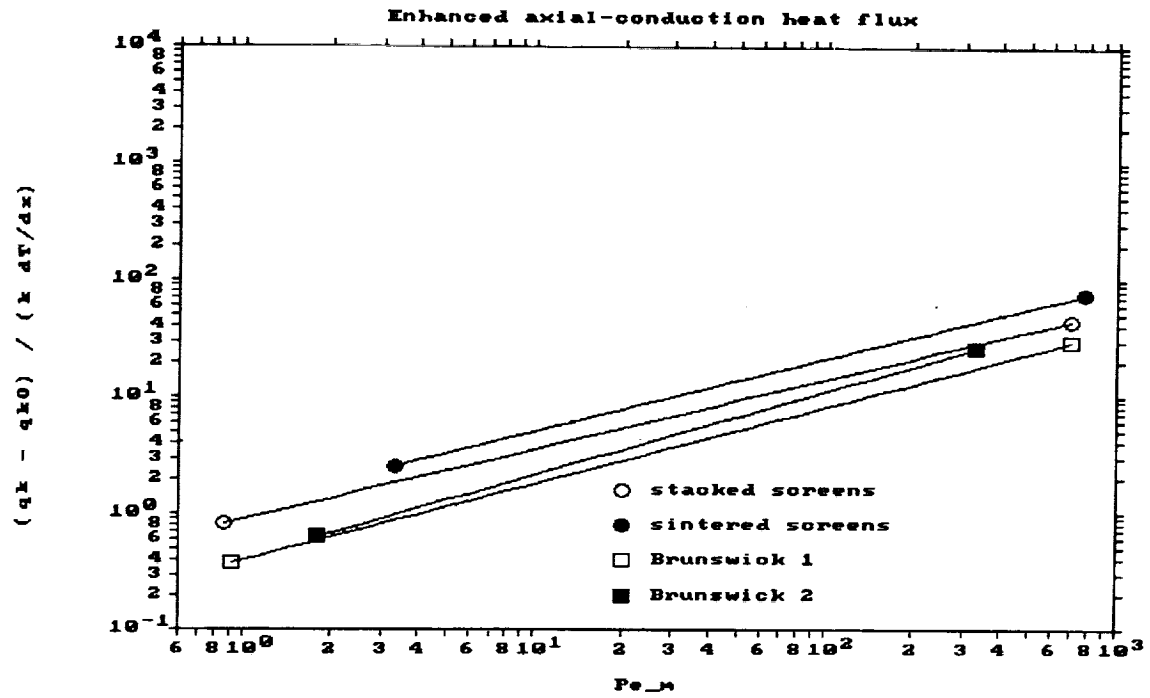
14

Figure 5: Contribution to net regenerator heat flux by enthalpy transport (q_h) compared to that of enhanced axial conduction $(q_k - q_{k0})$ for the four test samples.

According to our correlation forms, both N_u and $N_k - N_{k0}$ approach zero as P_e approaches zero. This is reasonable for $N_k - N_{k0}$ since it correlates the enhancement of conductivity over molecular conduction, which should vanish in the limit. But, based on laminar solutions in simple geometries, N_u should tend to some fixed non-zero value as P_e approaches zero. So our correlation form is theoretically wrong; it should include a constant term. But, practically speaking, it doesn't matter since axial conduction dominates regenerator heat flux at low P_e anyway. But in an application where the correct N_u is important at P_e near or below 1, our correlation will probably under-predict N_u, resulting in too large film temperature differences for a given rate of heat transfer. Fortunately, stirling regenerators seem to spend most of their time well above $P_e = 1$. In fact, according to Seume and Simon's survey paper [11], stirling regenerator are unlikely to operate below $R_{em} \approx 30$ ($P_{em} \approx 20$).

6 Test Details

We now turn to a discussion of the experimental and computational details that went into the correlations tabulated above. Once the experimental data points are logged, the data reduction work begins. The experimental can of worms now becomes a theoretical can of worms. Seemingly straight-forward data reduction leads to several open-ended questions.

6.1 Pressure-Drop Tests

Pressure-drop testing is relatively straight forward, involving only a measurement of sample pumping dissipation inferred from the PV work done by the piston. The principal uncertainties are due to the compressibility of the working gas when pressure-drop is large.

6.1.1 Data Files

For logbook cross-referencers, the original .RAW data file names for the four samples under pressure-drop testing were:

stacked screens:	2-03-02C, 2-03-30A, ..., 2-03-30C
sintered screens:	2-03-24A, ..., 2-03-24D, 2-03-25A, ..., 2-03-25C
Brunswick 1:	2-03-10A, ..., 2-03-10C , 2-03-10D, ..., 2-03-10F
Brunswick 2:	2-03-25D, ..., 2-03-25F , 2-03-25G, 2-03-25H

The numerical part of the above file names record the run date in year-month-day form (2 is short for 1992). The letter suffix distinguishes individual data points on a given date. After screening, translating, combining, the final .DRV file names were:

stacked screens:	s03-30NH
sintered screens:	s03-24NH
Brunswick 1:	s03-10NH
Brunswick 2:	s03-25NH

6.1.2 Error Analysis

In data modeling parlance, residuals measure the fit of our model to the experimental data and tell us much about the validity of what we have done. This information cannot be directly plotted on our friction factor curves because our experimental *measurable* is not instantaneous pressure drop but, rather, cycle-mean sample pumping dissipation. So we need separate residual plots, which the data modeling software cranks out each time it runs.

A number of these residual plots are condensed into figure 6. Inspection of these plots shows some interesting points. First, the residuals are normalized

17

so that we expect them to fall between $\pm$ 1, provided our error estimates are valid. (Pumping dissipation error estimates are based on our estimated errors for fast-pressure and piston-displacement measurements.) And, indeed, most residuals do seem to fall in this range. Second, any systematic deviation of our friction factor model from reality is evident as a non-random component to the residuals. We definitely see this, but the deviation remains within the error bounds we have a priori estimated. This suggests that the basic Ergun form for friction factor is quite good enough over a wide range of Reynolds numbers. Third, we can spot non-repeatable trends in our experimental measurements by patterns or clusters in the residuals. We see this in our plots as regular traces superimposed on the average systematic deviation. But again, these clusters represent errors within our expected $\pm$ 1 error band, so we are not worried about them. Evidently, there is much to the study of residuals, and one could easily devote his life to reading such entrails.

The only other error worth considering in pressure drop testing is the error in the model-predicted pumping dissipation as a result of variations in mass flux g across the test sample. Mass flux varies because of time-dependent density variations resulting from the pressure swing in the cylinder. The pressure-drop data modeling software produces an error plot which estimates the relative magnitude of this error. This error was small for all samples tested.

6.1.3 Comparison to Other Data

Published data for friction factors in steady porous flow is relatively common. Oscillating-flow results are much rarer, but this does not worry us too much because of the negligible role Valensi number (measure of dimensionless frequency) seems to play in our data. We will demonstrate this later. For comparison purposes we used results reported for nominally the same materials in table 7.2-1, p 181, of NASA oscillating-flow report [9], and for similar materials in figure 7-9, p. 149, of Kays and London [7].

Figure 7 compares present screen results against those in the NASA report. While friction factors are close in the range of common Reynolds number, there are differences. The steady-flow data suggests that stacked-screen friction factors are greater than sintered-screen values. Our present data suggest that friction factors are about the same for both, and midway between the two steady-flow values. These discrepancies may be attributable to experimental errors, or to variability in the packing and sintering process, which we understand is potentially considerable. We may never know. We, of course, favor the present results.

Because of the lack of an analytic formulation for the Kays and the London data, we have not plotted a comparison of the present screen friction factors with their data. However, if we spot check our stacked screen friction factors against their closest-comparison screen of porosity 0.602, we find reasonable agreement in the range $8 < R_e < 2000$, as the following table shows. When
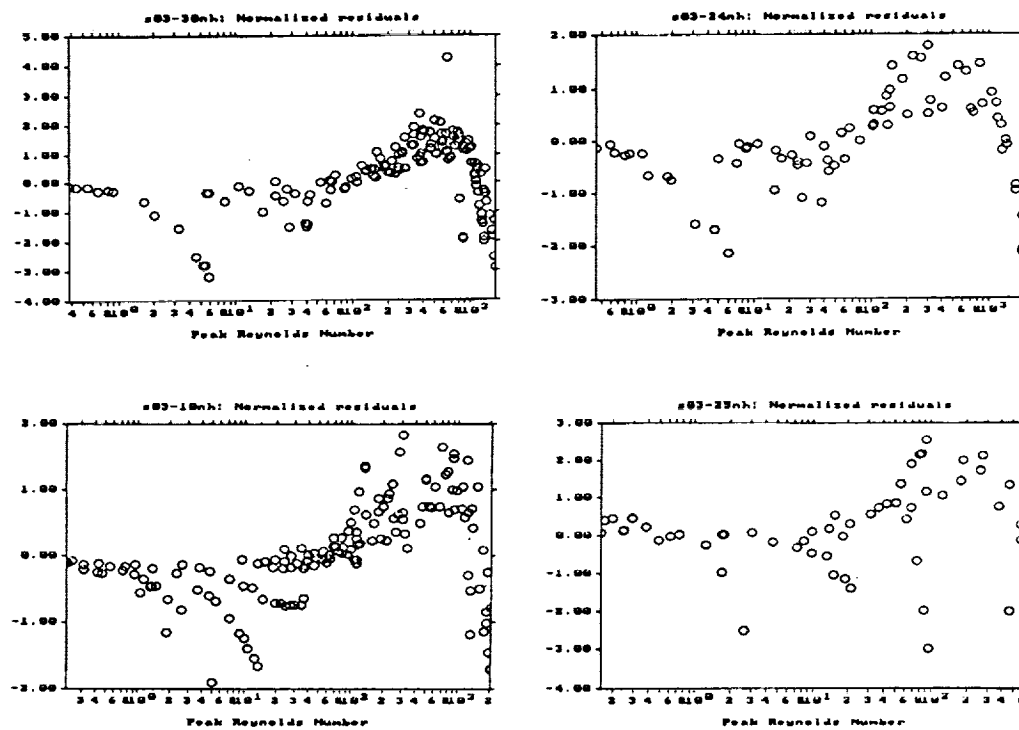
18

Figure 6: Residuals for friction-factor parameter estimates: stacked screens (upper left), sintered screens (upper right), Brunswick 1 (lower left) Brunswick 2 (lower right)
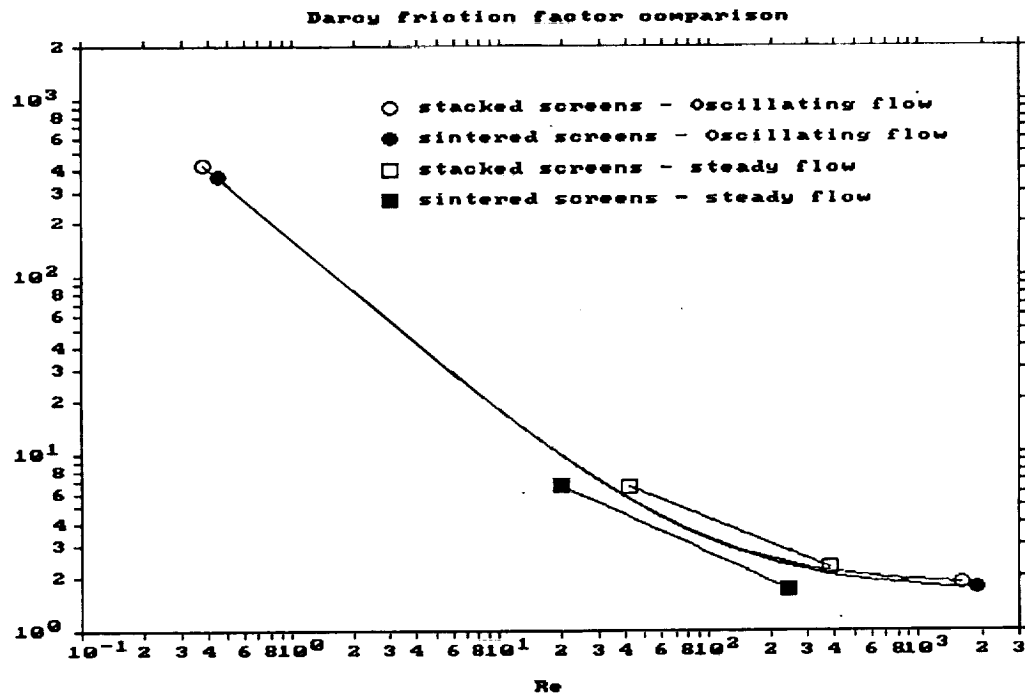
19

Figure 7: Comparison of oscillating-flow friction factors of the present study with steady-flow values reported in the NASA oscillating flow report

comparing our Darcy friction factors to Kays and London's Fanning factors we must always remember to multiply by 4.

R_e	8	20	60	100	400	1000	2000
f — stacked screens	21.6	9.69	4.39	3.33	2.14	1.90	1.82
f — Kays & London	29.2	13.0	5.90	4.60	2.72	2.14	1.87

Although porosity was similar in this comparison, the 280 micron wire diameter of the Kays and London sample was much larger than the 53 micron diameter in our sample.

6.2 Heat-Transfer Tests

As its principal experimental variable, heat transfer testing measures net heat flux down the regenerator inferred from cooler heat rejection less PV power and heat leaks. Compared to pressure-drop testing, this is more complicated, time consuming, and noisier; the noise being chiefly due to the rather large and time-varying nature of heat leakage.

6.2.1 Data Files

The original .RAW data file names for the four samples under heat-transfer testing were:

stacked screens:	2-05-14A, ..., 2-05-14E, 2-05-15A, ..., 2-05-15C
sintered screens:	2-05-06A, 2-05-07A, 2-05-07D, 2-05-07F, 2-05-07H, ..., 2-05-07J, 2-05-07L, 2-05-08A
Brunswick 1:	2-05-25C, ..., 2-05-25F , 2-05-26D
Brunswick 2:	2-05-21B, ..., 2-05-21H

And, after screening, translating, combining, the final .DRV file names were:

stacked screens:	NH05-14
sintered screens:	NH05-07
Brunswick 1:	NH05-25
Brunswick 2:	NH05-21

6.2.2 Error Analysis

In heat-transfer parameter estimation the residuals measure the net regenerator heat flux discrepancy between the experimental data points and the theoretical model. We evaluated several theoretical models depending on which of N_q, N_u, N_k or N_{ue} we were attempting to correlate, and the functional form of the correlation. But in all cases the residuals turned out about the same. The plots all looked similar and the best-fit chi-squared value (sum of squares of

normalized residuals) was always within about $\pm$ 10% of the same value for a given data set.

This suggests not so much that our theoretical models were all uniformly excellent, but rather that the random experimental noise in our data was relatively large. The noise was probably obscuring the fit of our models to the data. Said in another way, had experimental noise been smaller, the degree of fit of our models to the data would have been more apparent.

Figure 8 shows residual plots for simultaneous N_u and N_k parameter estimation according to equations (2) and (3). The same figure applies pretty well to all other heat-transfer parameter estimations.

The heat-transfer data modeling software also produces a number of other error plots. Displayed on the console are plots of

1. Signal to estimated-noise ratio

2. Relative error induced by g error

3. Relative error induced by T error

4. Relative error induced by neglected terms

All these plots are normalized by our advance estimates of regenerator heat-flux measurement noise, which seem roughly consistent with the actual random error observed. All the relative-error plots were previously discussed in the SBIR phase I report [4].

Plots of type 1 show us the relative significance of noise in our data. High signal-to-noise ratios are, of course, good for reliable data modeling. And, for the most part, our data does enjoy a high signal-to-noise ratio as is shown in figure 9. Data at low Peclet numbers is the exception to the rule.

Plots of type 2 show the effect on modeled regenerator heat flux of estimated errors in mass flux g. Both g and its error estimate come from GLIMPS simulation — g being the mid-sample value and its error being the variation in g across the sample. In all cases, g-induced relative errors were small so they do not appear in this report.

Plots of type 3 show the effect on modeled regenerator heat flux of estimated errors in the presumed-constant sample midpoint temperature gradient $\frac{\partial T}{\partial x}$. All models predict linear variation of regenerator heat flux with $\frac{\partial T}{\partial x}$. The error estimate for $\frac{\partial T}{\partial x}$ is based on instrumentation error and local temperature variations related to solid-to-gas heat capacity ratio and flow tidal amplitude. Figure 10 shows these errors for our data. The errors tend to grow with peak Reynolds number but always remain acceptable.

Plots of type 4 show the effect on modeled regenerator heat flux of key neglected terms in the model such as: the component of solid temperature variation that contributes to net enthalpy flux, time-varying pressure, spatially-varying mass flux and spatially-varying axial conduction. These errors only
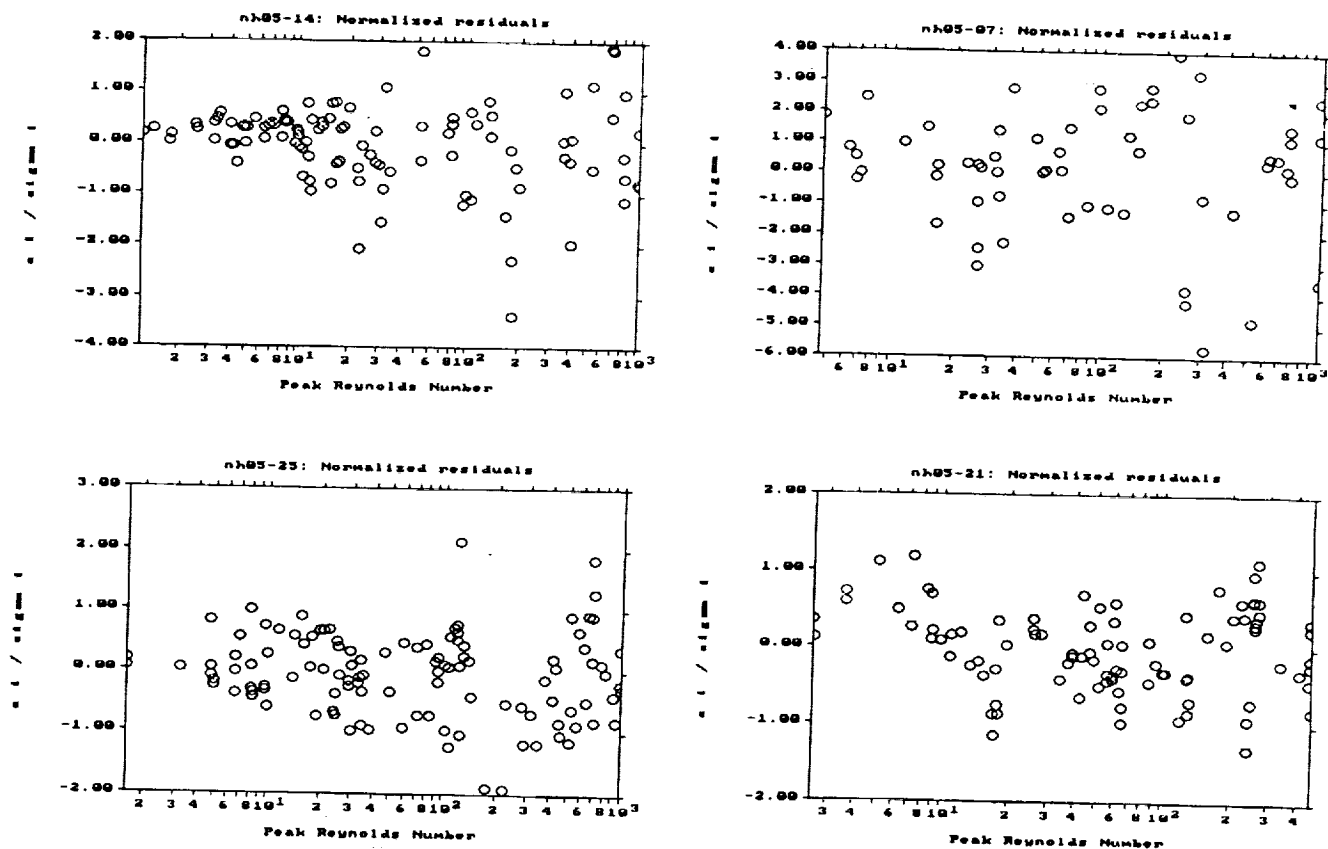
22

Figure 8: Residuals for heat-transfer parameter estimates: stacked screens (upper left), sintered screens (upper right), Brunswick 1 (lower left) Brunswick 2 (lower right)
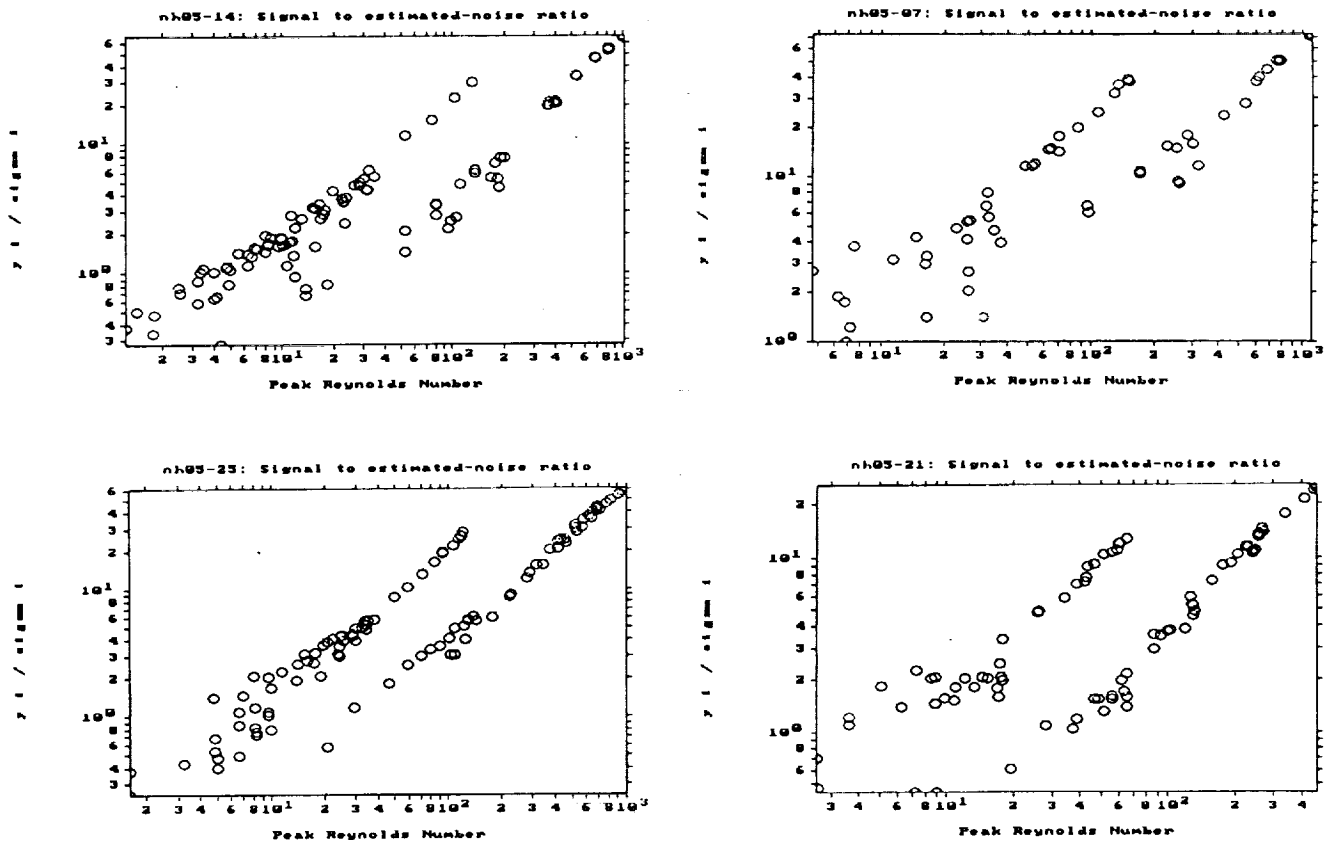
Figure 9: Signal to estimated-noise ratios for heat-transfer data sets: stacked screens (upper left), sintered screens (upper right), Brunswick 1 (lower left) Brunswick 2 (lower right)
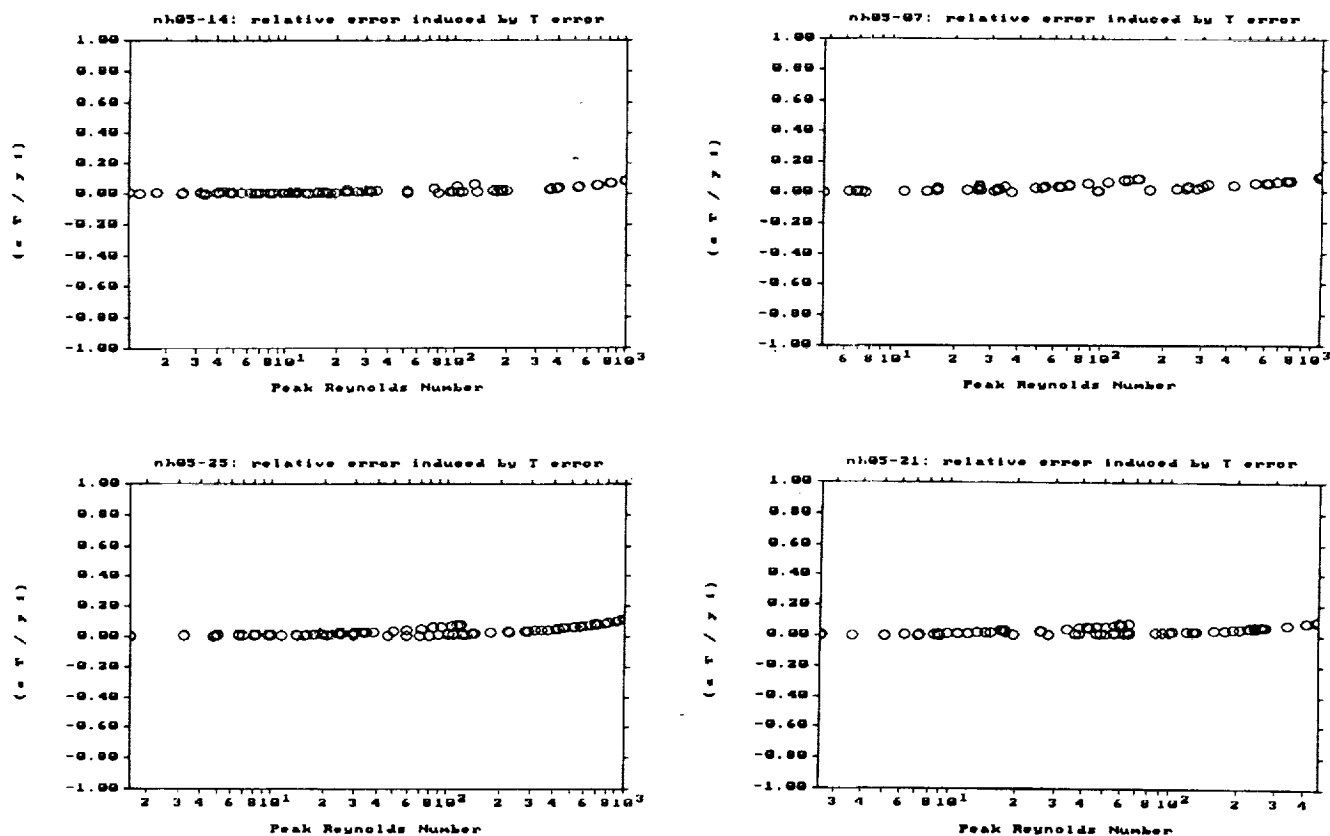
Figure 10: Relative error induced by non-constant mid-point $\frac{\partial T}{\partial x}$ for heat-transfer data sets: stacked screens (upper left), sintered screens (upper right), Brunswick 1 (lower left) Brunswick 2 (lower right)

pertain to models correlating N_u, N_k or N_{ue}, not to those correlating overall heat flux N_q. In some cases these errors are significant as is shown by figure 11.

Disturbed by these relatively large neglected-term error estimates, especially in the Brunswick data, we decided to investigate further. The question is whether or not data points with high neglected-term errors are tainting our parameter estimates. To directly check this we split the Brunswick 1 data set NH05-25 into two disjoint pieces: NH05-25L with neglected-term errors below about 20% and NH05-25H with errors 20% and above. We estimated parameters for effective Nusselt number N_{ue} separately for the two data sets. Figure 12 shows the results. The good agreement in the overlap region between $30 < P_{em} < 400$ shows that parameter estimates are only weakly affected by neglected-term relative errors on the order of 20 – 30% This would seem to say our error estimates are conservative, which is good.

6.2.3   Comparison to Other Data

Good published data for heat-transfer properties in porous materials is scarce. We have relied on one source for our comparisons: Kays and London [7], for woven-screen matrices. However, their tests were for steady flow with data reduction based on tracking a step temperature changed downstream of the sample matrix, neglecting axial thermal diffusion. We are willing to ignore the differences between steady and oscillating flow because of reasons to be cited below. However the assumption about axial thermal diffusion quite critical. Our results suggest that this omission will introduce progressively larger errors into their data reduction methodology as Peclet (Reynolds) number gets below about 10.

The assumptions behind the Kays and London correlations are consistent with our method of reducing N_{ue} assuming $N_k - N_{k0} = 0$. Therefore, we use this as a basis of comparison. However, both methods are likely to suffer from error at low Peclet numbers, and the errors may not be the same. Figure 13 seems to bear this out, showing that our N_{ue} predictions agree well with Kays and London at high Peclet numbers but not so well at the low end of the scale. We feel our estimate is likely to be more accurate for stirling-cycle use since it is designed to correctly predict net heat flux down the regenerator, while the Kays and London technique does not address this issue. The actual comparison correlation for Kays and London is the best-fit analytic expression found in the GLIMPS manual, with porosity dependence built in.

On the matter of comparing with others our overall heat-flux (N_q) estimates, or our simultaneous N_u and N_k estimates, we seem to be out of luck. We are unaware of any published data upon which to base a comparison. After all, we are breaking new ground here.
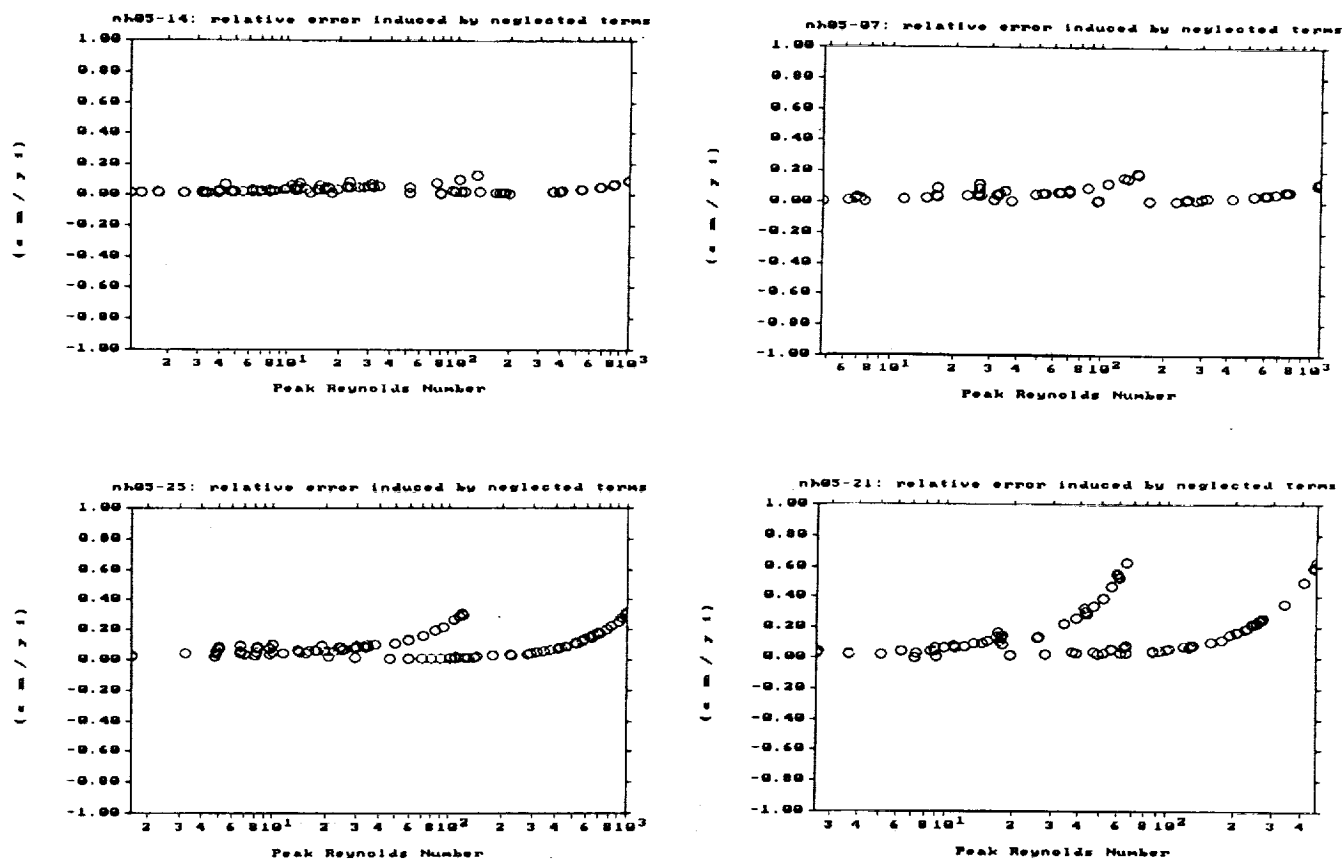
26

Figure 11: Relative error induced by neglected terms in model for N_u and N_k parameter estimates: stacked screens (upper left), sintered screens (upper right), Brunswick 1 (lower left) Brunswick 2 (lower right)
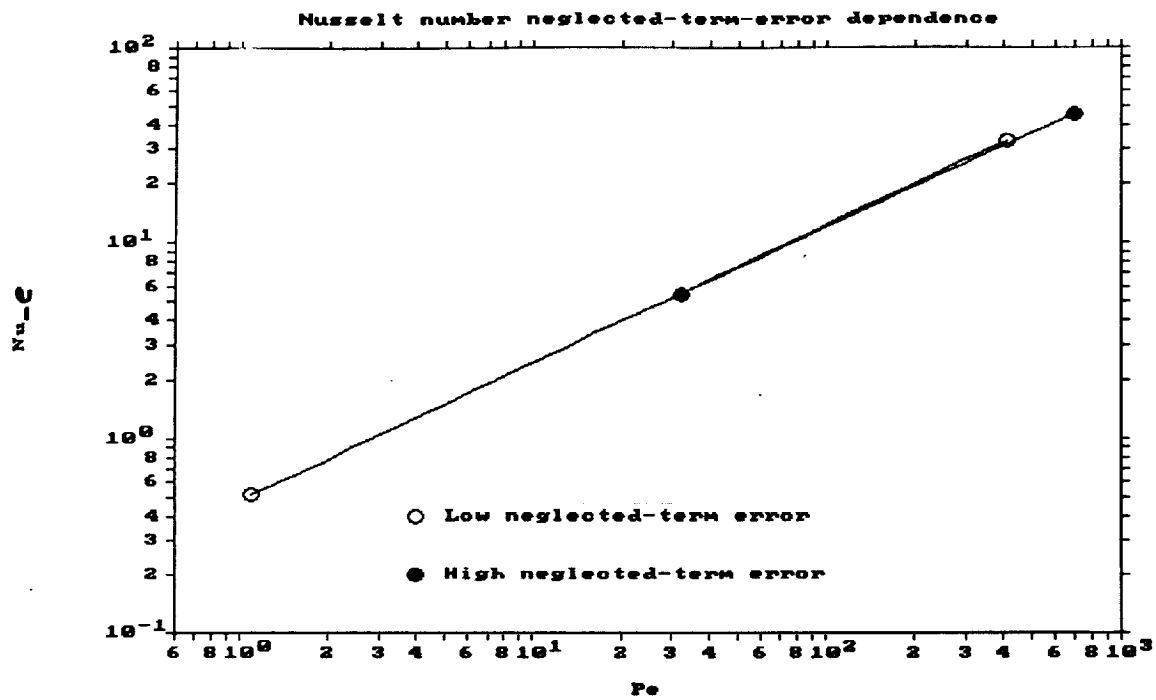
27

Figure 12: The Brunswick 1 data set broken into two disjoint pieces with low and high neglected-term errors and reduced separately.
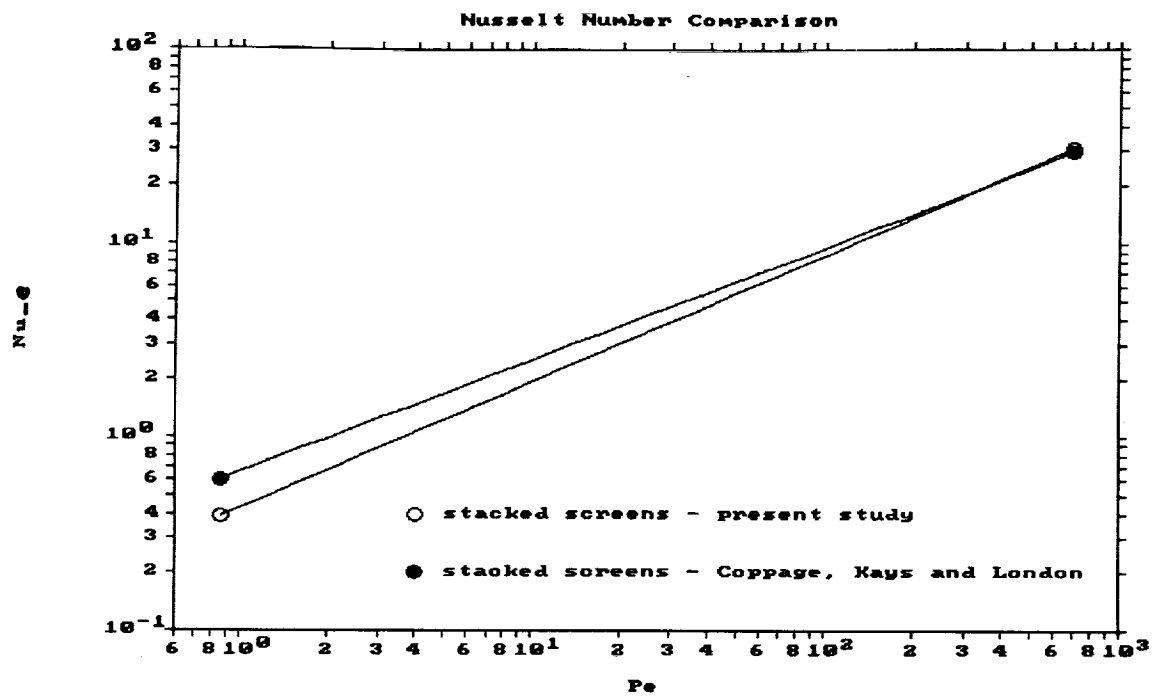
Figure 13: Comparison of our stacked-screen effective Nusselt number correlation (neglecting enhanced axial conduction) with Kays and London values

6.3 Evaluating Model Completeness

The issue here is whether our expressions for f, N_u, N_k, N_{ue} and N_q can be correlated solely in terms of Reynolds (Peclet) number, or must we bring into play other dimensionless groupings such as, in particular, Valensi number or tidal amplitude ratio. Oscillating duct-flow research has thus far identified both Reynolds number and Valensi number as key players. However, compared to heat exchanger ducts, Valensi numbers are typically quite low in regenerator-matrices, owing to their small hydraulic diameters. Therefore, the consensus among oscillating flow researchers has been that we are unlikely to see much Valensi-number dependence in typical stirling regenerator matrices tested under typical stirling conditions. And tidal amplitudes, while often small compared to the total sample length, are usually quite large compared to the mean pore size. Therefore, it follows that the distance required to fully develop porous flows is much less than typical tidal amplitudes, so that we do not expect to see any tidal amplitude dependence either. Our present tests bear out the above presumptions.

We maintain that some sort of Reynolds analogy holds between heat transfer and flow friction so that it is only necessary to investigate one or the other for dependence on alternate dimensionless groups. We chose to investigate friction-factors rather than N_u, N_k N_{ue} or N_q. This was partly because pressure-drop tests came first and partly because pressure-drop measurements are not as noisy as heat transfer measurements.

6.3.1 Valensi Number Independence

First, the case for Valensi number. We split the packed-screen nitrogen data set S03-02C into two disjoint subsets — a low V_a subset and a high V_a subset. The first subset contained all data points with V_a below the median of the total data set and the second subset contained all data points with V_a above. We then ran both subsets though the data modeling process. Figure 14 shows the results. One can see that friction factors show little dependence on Valensi number, especially at high Reynolds numbers around 1000. At intermediate Reynolds numbers around 100, there seems to be some evidence for increased friction factor at high Valensi numbers, but the effect is small (about 10%) and may be an artifact of data modeling rather than a real difference. Our conclusion is that, based on this data, we are justified in ignoring friction factor Valensi number dependence. However, we should be cautious in applying this conclusion to data sets where Valensi number is significantly greater than the 3.72 maximum for the present set.

6.3.2 Tidal Amplitude Independence

We repeated this exercise for tidal amplitude ratio. We again divided the same packed-screen data set into two disjoint halves, this time sorted by tidal ampli-
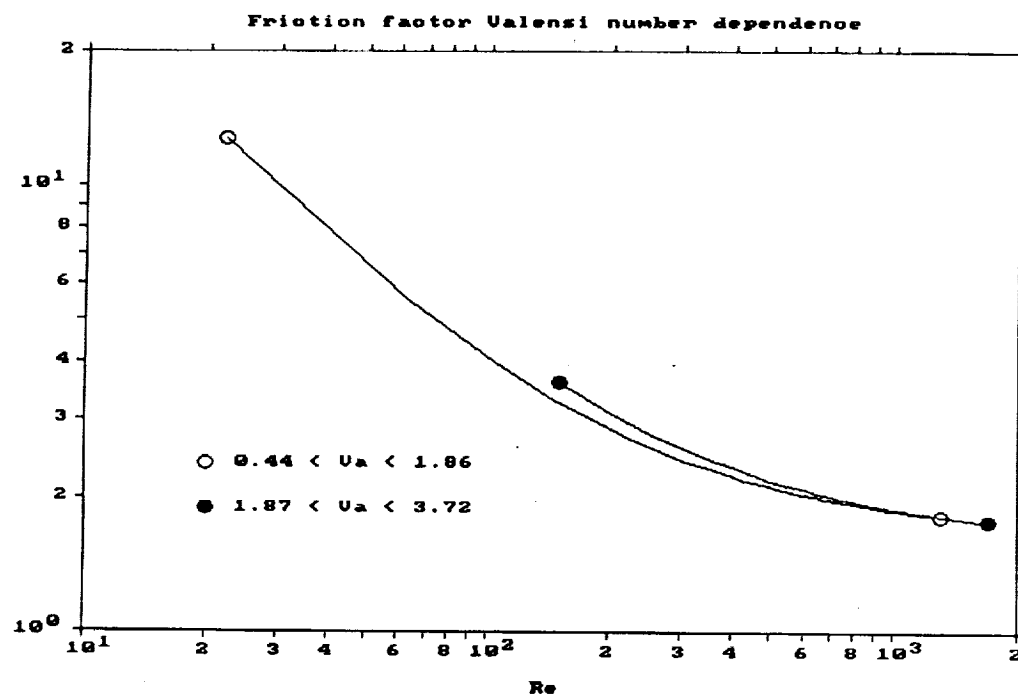
Figure 14: The packed-screen nitrogen data set broken into low and high Valensi number halves and reduced separately
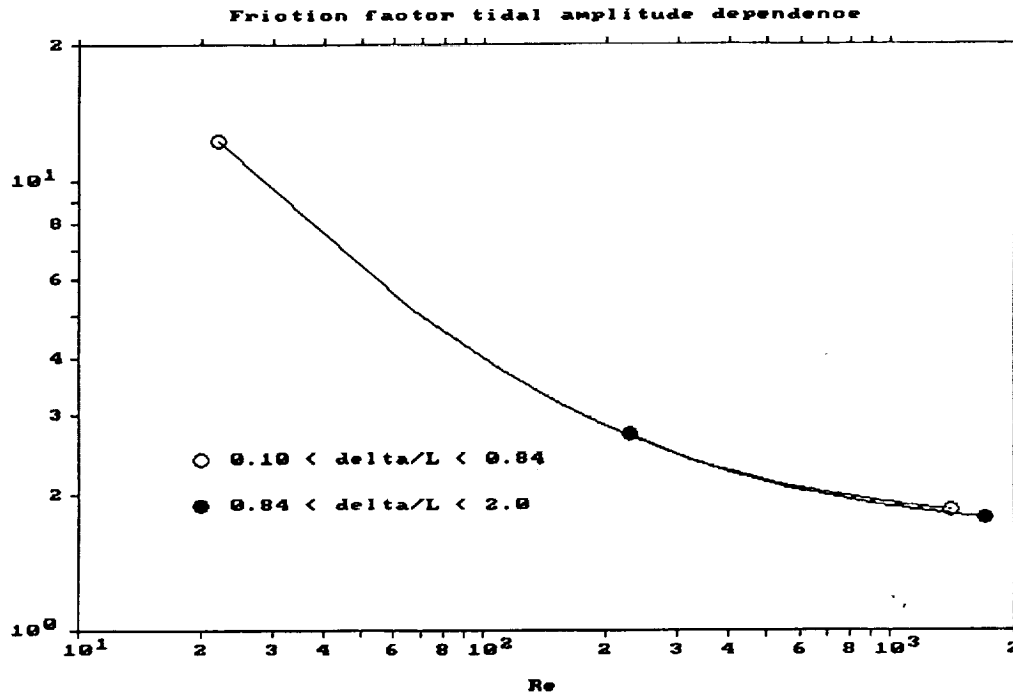
Figure 15: The packed-screen nitrogen data set broken into low and high tidal amplitude halves and reduced separately

tude ratio. Figure 15 compares the low and high δ/L friction factors. There is no significant difference between the two curves in the region of overlap. This seems to confirm that developing flow or entrance-region effects are negligible in this sample.

6.3.3 Working Gas Independence

Another issue is that of working-gas independence. All of our theoretical analysis is based on dimensionless groupings and so we expect to see no dependence on the particular dimensional properties of the working gas. However, having said that, it is always prudent to check. Were we to actually see a dependence on working gas it would probably point to an experimental measurement error or, possibly, some as-yet-undiscovered dimensionless group of importance (Mach number, compressibility, etc).

So we once again split up a data set into two halves — this time for the Brunswick 1 sample, divided according to whether the working gas was helium or
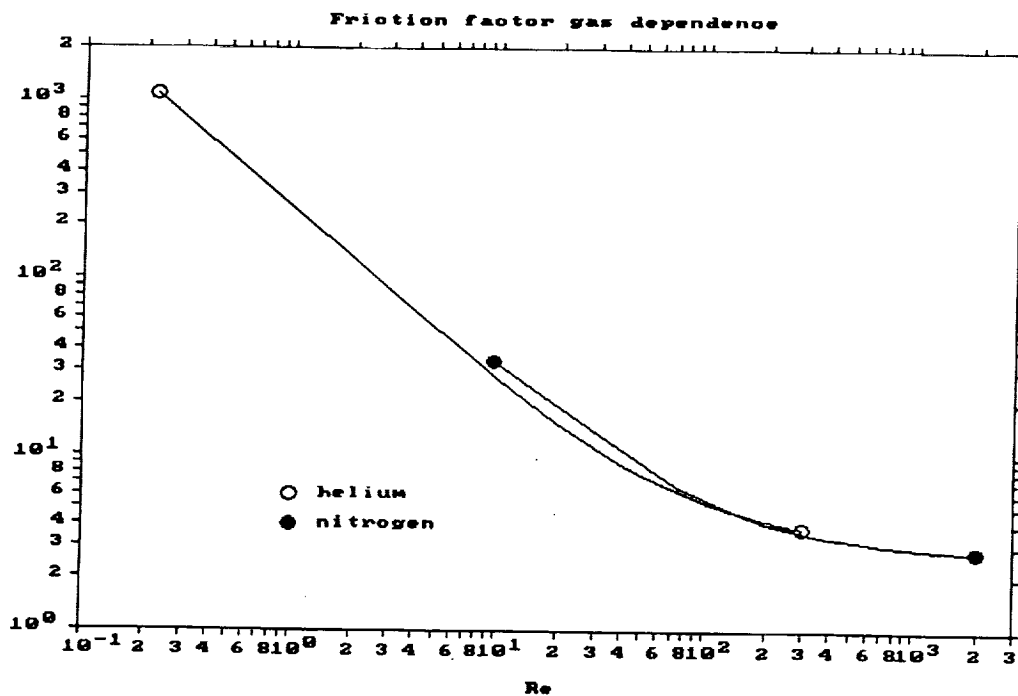
32

Figure 16: The Brunswick 1 data set broken into nitrogen and helium pieces and reduced separately

nitrogen. Figure 16 compares nitrogen-derived friction factor to helium-derived friction factor. We see that the curves are reasonably close in the range of common Reynolds number. This casts a vote of confidence in our experimental measurements and further suggests that no relevant dimensionless groupings have yet to be uncovered.

7 Conclusions and Recommendations

We have correlated expressions for pressure-drop and heat-transfer characteristics in four test samples representative of typical stirling-cycle regenerators. Even though much of this information is new, we are comfortable in recommending it for use by stirling-cycle modelers in its current form. Our error analysis and comparisons to the work of others, suggest that the correlations are quite accurate — certainly more accurate than anything else publicly available. An exception to this might be the estimates for enhanced axial conductivity ratio N_k for which our error bands remain a bit broad. However, we hope to improve our these estimates in the future and, besides, stirling modelers will still get the correct value for net regenerator heat flux, even if N_k is a bit off.

We have also provided compelling evidence that correlating pressure-drop or heat-transfer expressions solely in terms of Reynolds or Peclet number is sufficient for stirling-cycle purposes. We need not worry about the banes of oscillating flow, Valensi number, tidal amplitude, entrance effects or other complicating dimensionless groupings.

We are well on our way toward achieving general-purpose correlations for use by stirling modelers. But we are not quite there yet. We would eventually like correlations that apply over an entire class of regenerator matrices, rather than one specific instance. For example, we would like a single correlation for all screens, one that would include a term for porosity dependence, rather than a set of correlations for individual screen matrices. Likewise for all Brunswick random round-wire regenerators, or all random non-round-wire regenerators, etc. To achieve these goals we must test more screen regenerators and more Brunswick regenerators over a wide range of porosities.

We also need to keep an open mind to alternate correlating expressions for N_u and N_k — especially if we ever manage to significantly reduce our heat-flux measurement errors. In particular, we need to devote more thought to the limiting constant value for N_u as P_e tends to zero.

On the experimental front we have identified the following general goals as key to improving the accuracy of our final correlating expressions:

- Boost signal-to-noise ratio in heat-transfer tests by some combination of reducing static conduction, shortening the sample, increasing the sample temperature difference, improving resolution in coolant mass flow measurements or investigating a closed-loop coolant system

- Improve estimated parameter confidence bands by increasing the number of data points logged per sample and weighting data points toward the Reynolds number extremes

The first goal would be most helpful in sorting out N_k and N_u at the low end of the Peclet number range.

References

[1] J.P. Holman, *Heat Transfer, 4th Edition*, McGraw-Hill, (1976)

[2] C.T. Hsu and P. Cheng, *Thermal dispersion in a porous medium*, Int. J. Heat Mass Transfer, Vol. 33, No. 8, pp. 1587–1597, (1990)

[3] M.F. Edwards and J.F. Richardson, *Gas Dispersion in Packed Beds*, Chem. Eng. Sci., Vol. 23, pp. 109–123, (1968)

[4] D. Gedeon, G. Koester and Al Schubert, *A Test Rig for Measuring the Thermal Performance of Stirling Cycle Regenerators*, SBIR Phase I report, Sunpower Inc., NASA Lewis contract NAS3-25620, (1989)

[5] D. Gedeon, *Why N_u and N_k Should Vary Similarly with R_e*, personal memorandum, December 17 (1991)

[6] J.P. Holman, *Heat Transfer*, Fourth Edition, McGraw-Hill (1976)

[7] W.M. Kays and A.L. London , *Compact Heat Exchangers*, Third Edition, McGraw-Hill (1984)

[8] W.M. Kays, *Convective Heat and Mass Transfer*, McGraw-Hill (1966)

[9] G. Koester, S. Howell, G. Wood, E. Miller, D. Gedeon, *Oscillating Flow Loss Test Results in Stirling Engine Heat Exchangers*, NASA Contractor Report 182288, (1990)

[10] I.F. Macdonald, M.S. El-Sayed, K. Mow and F.A.L. Dullien, *Flow through Porous Media – the Ergun Equation Revisited*, Ind. Eng. Chem. Fundam., Vol. 18, No. 3, pp. 199–208, (1979)

[11] J.R. Seume and T.W. Simon, Oscillating Flow in Stirling Engine Heat Exchangers, 21st IECEC, American Chemical Society, pp. 533–538, (1986)